

Latent analysis of unmodified biomolecules and their complexes in solution with attomole detection sensitivity

Emma V. Yates,[†] Thomas Müller,[†] Luke Rajah,[†] Erwin J. De Genst,[†]
Paolo Arosio,[†] Sara Linse,[‡] Michele Vendruscolo,[†] Christopher M. Dobson,^{*,†} and
Tuomas P.J. Knowles^{*,†}

Department of Chemistry, University of Cambridge, Lensfield Road, Cambridge, CB2 1EW, United Kingdom, and Department of Biochemistry and Structural Biology, Lund University, SE221 00 Lund, Sweden

E-mail: cmd44@cam.ac.uk; tpjk2@cam.ac.uk

Phone: +44 (0)1223 336344

Abstract

The study of biomolecular interactions is central to an understanding of function, malfunction, and therapeutic modulation of biological systems, yet often involves a compromise between sensitivity and accuracy. The conventional analytical steps and the procedures required to facilitate sensitive detection, such as the incorporation of chemical labels, are prone to perturb the complexes under observation. Here we present a ‘latent’ analysis approach which uses chemical and microfluidic tools to reveal, through highly sensitive detection of a labelled

*To whom correspondence should be addressed

[†]University of Cambridge

[‡]Lund University

system, the behaviour of the physiologically relevant unlabelled system. We implement this strategy in a native microfluidic diffusional sizing platform, allowing us to achieve detection sensitivity at the attomole level, determine the hydrodynamic radii of biomolecules that vary by over three orders of magnitude in molecular weight, and study heterogeneous mixtures. Utilising these key advantages we characterised a complex of an antibody domain, in the solution phase and under physiologically relevant conditions.

Protein-protein interactions are central to the framework with which biological systems respond to their environments over a range of temporal and spatial timescales.¹⁻⁶ Rapid and transient interactions in particular allow a system to react to a stimulus in a coordinated and complex fashion, using a limited number of components. Moreover, such interactions are increasingly recognised as a key target for the design of more selective pharmaceuticals which modulate, rather than broadly inactivate, their targets.⁷ This approach – and indeed, the general aim of probing protein-protein interactions under physiologically relevant conditions – remains highly challenging, in part because many of the assays themselves have the potential to perturb the interactions under observation.^{8,9}

Common methods for studying protein-protein interactions include two-hybrid screens,¹⁰ mass spectrometry,¹¹ protein microarrays,¹² and surface plasmon resonance (SPR) techniques such as BIAcore. However, fusion or immobilisation, or transfer into the gas phase raises the possibility that the conformational ensemble sampled by the protein of interest may not mimic that explored under native conditions.⁹ Solution phase methods such as analytical ultracentrifugation (AUC), isothermal titration calorimetry (ITC), nuclear magnetic resonance (NMR),¹³ and static and dynamic light scattering (DLS) can overcome this limitation, but often require concentrations exceeding the biologically relevant range and consume large amounts of protein or require specialised equipment.¹⁴ Good detection limits have also been attained with native fluorescence capillary electrophoresis (NCE)¹⁵ when the intrinsic fluorescence of the sample is high, and backscattering interferometry (BSI)¹⁶ when factors other than binding events, which may cause a measurable change in refractive index, are precisely controlled.

Alternatively, a general and cost effective method to increase the sensitivity is via the incorporation of protein or small molecule labels, such as fluorescent dyes, but even with careful choice of the labelling position these can introduce artefacts into the measurement by affecting the conformational ensemble of the protein studied.¹⁷ Conventionally, if the protein is modified in some way – such as through the installation of a fluorescent protein or small molecule label – to permit sensitive detection, then the experiment is capable of revealing exclusively the behaviour of the modified protein, which may differ from that of the natural system. We present a new approach, that we define to be ‘latent,’ because the labelling is instead a component of the measurement process, in a manner such that it is unable to perturb the biological process under observation (**Fig. 1a**). Latent labelling exploits the ability to spatially separate reaction chambers within a microfluidic system operating under steady state flow conditions, and continuously direct native, unmodified biomolecules with desirable properties to a chemically distinct region of the microfluidic system, where they are labelled with a fluorogenic molecule prior to the detection step (**Fig. 1a,b**). We exploit microfluidic and chemical tools to ensure that the behaviour of the unlabelled, physiologically relevant system can be extracted from the simple optical detection of the labelled system.

We demonstrate that biomolecules can be quantitatively labelled in seconds, with a fluorogenic dye under denaturing conditions, on a microfluidic chip. We incorporate this latent labelling module into a native microfluidic diffusional sizing system. Using this technique, it is possible to detect even attomole quantities of biomolecules, while studying the behaviour of unlabelled biomolecules and their complexes under fully native solution conditions through measuring, and assessing changes in, sample hydrodynamic radius (R_H). We show that biomolecules ranging in molecular weight (MW) by over three orders of magnitude can be accurately sized without the need for a calibration step, and therefore that this approach exceeds the dynamic range of existing techniques. We further demonstrate that the technique tolerates both intrinsically disordered proteins and heterogeneous mixtures, and demonstrate the power of the method to characterise a clinically relevant α -synuclein immune complex. These results suggest that native microfluidic diffusional sizing, and indeed additional applications of the latent labelling approach, will become valuable

tools for the characterisation of biomolecules and their complexes, under fully native conditions and over a wide range of concentrations and timescales, and further, for the investigation into how such interactions can be modulated.

Results and Discussion

Latent labelling and its integration into microfluidic systems

At a fundamental level, the measurement process consists of preparing a system in a well-defined initial state, monitoring its time evolution under a set of conditions governed by a parameter of interest, and then detecting that time evolution through a change in some observable. If a label is installed to increase detection sensitivity, then the measurement reveals exclusively the behaviour of the labelled system (**Fig. 1a**). We have used chemical and microfluidic tools to design a latent labelling strategy which decouples these steps of the measurement process, spatially and chemically, by confining them to distinct reaction chambers within a microfluidic system operating at steady state (**Fig. 1a,b**). Labelling enables highly sensitive detection, but the samples are unlabelled when the property of interest is probed via the time evolution step, so the label cannot affect the measured property.

Our approach exploits the distinct properties of fluid when confined to small (μm) length scales. When two streams of fluid, one containing biomolecules of interest and the other containing exclusively buffer, meet in a microfluidic channel, there is no convective mixing, and transport of the biomolecules into the buffer perpendicular to the direction of the flow lines proceeds, in the absence of an applied force, exclusively via diffusion.¹⁹ It is possible to separate reaction chambers in time by spatially separating them along the direction of flow within the microfluidic system. Biomolecules of interest can be partitioned between these chambers by orienting the chambers, perpendicular to the flow direction, such that exclusively biomolecules whose properties of interest fall within a desired range are able to flow along a particular path.^{20,21}

Here we couple our latent labelling strategy with a diffusional sizing approach. Advantages of

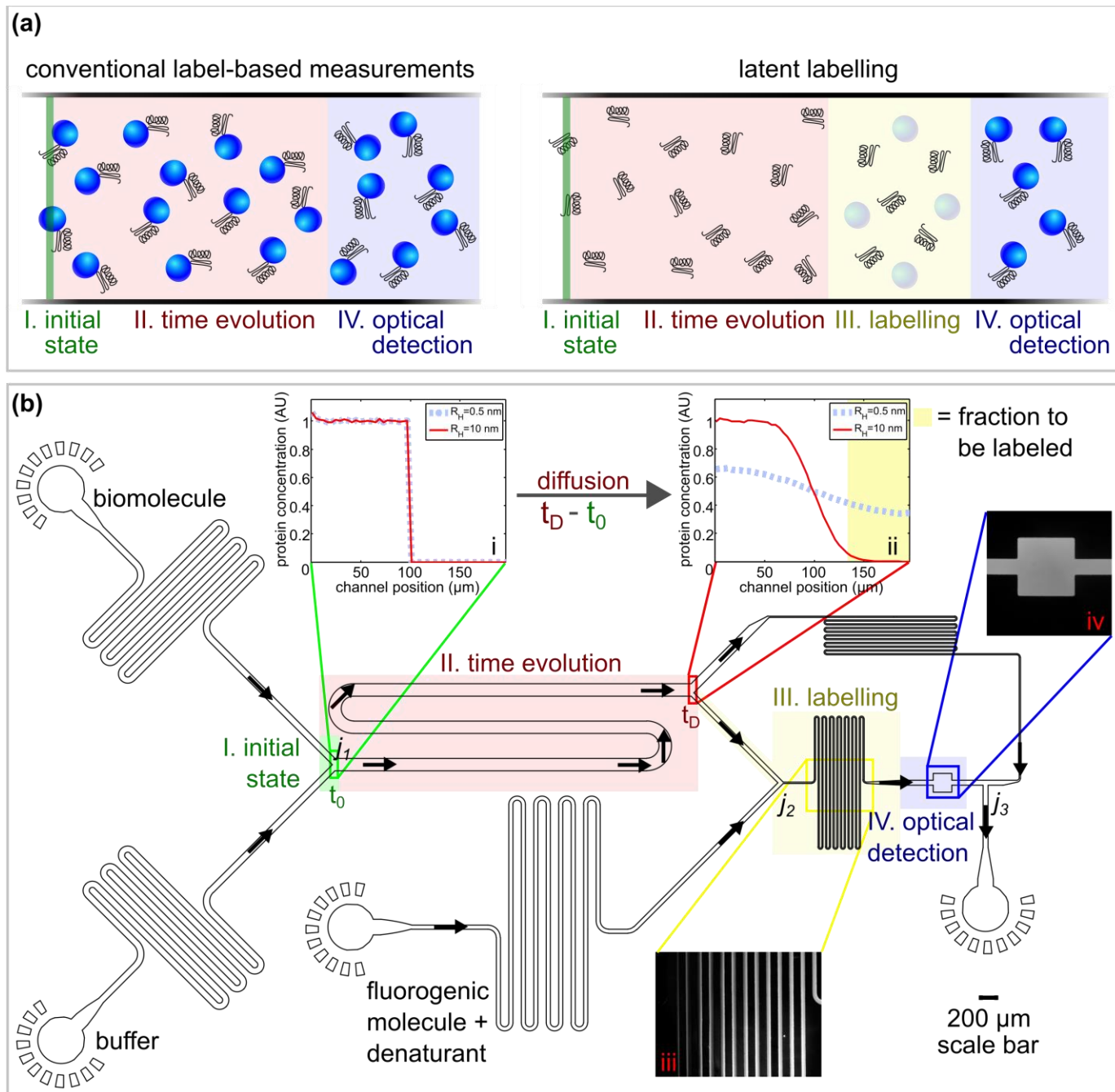


Figure 1: Latent labelling enables the development of native microfluidic analysis systems (a) While conventional measurements can involve a compromise between sensitivity and accuracy – the behaviour of labelled biomolecules (blue spheres) may differ from that of their unlabelled, physiological counterparts – the introduction of a latent labelling step within the measurement process enables sensitive optical detection of labelled biomolecules to provide a snapshot of the time evolution of the native biomolecules. Under well-controlled laminar flow conditions in microfluidic systems, this time evolution can be related to fundamental physical properties such as charge¹⁸ or size. (b) To illustrate this, we have designed a native microfluidic diffusional sizing device. Arrows indicate the direction of fluid flow. Diffusion into a stream of buffer over time $t_D - t_0$ separates biomolecules according to their R_H . A well-defined fraction of the distribution (yellow rectangle) is selected and labelled via mixing with a fluorogenic molecule and denaturant (inset *iii*). Because labelling is quantitative (Fig. 2), optical detection of fluorescence intensity (inset *iv*) reveals the total concentration of biomolecules diverted for labelling, which reports on the size distribution of the native, unlabelled species at time t_D . Simulated distributions across the diffusion channel for particles of two known sizes are shown in inset *ii*.

this approach include that sizing is done in the solution phase, is non-invasive, is suitable for the study of complex mixtures, and is tolerant of a wide range of solution conditions. Biomolecular diffusion coefficients are determined by measuring the extent of mass transport perpendicular to the direction of flow, after a known residence time.²⁰⁻²⁴ In the microfluidic device (**Fig. 1b**), the first step of the measurement process is the establishment of a well-defined initial state: when the protein and buffer streams meet at time t_0 , no diffusion has taken place, so proteins of all R_H have the same initial distribution, laterally spanning half the width of the diffusion channel as the volumetric flow rates of the protein and buffer streams are equal. The system is then allowed to evolve for a defined period of time, $t_D - t_0$, after which the smaller species have diffused further than have the larger species. A simulation of the behaviour of two species, one with R_H of 0.5 nm and the other with R_H of 10 nm, is shown in insets *i* & *ii*. At this stage the biomolecule is unlabelled, so no direct observation of diffusion at time t_D occurs. Instead, molecules which have diffused at least one sixth the channel width in time $t_D - t_0$ (yellow rectangle) are diverted to the labelling module. The total concentration of labelled molecules (integrating the size-dependent distribution within the yellow rectangle) reports on the distribution at time t_D , and is thus used to determine molecular size (**Fig. 3a**).

We note the generality of the latent analysis approach. In the laminar regime, it is possible to choose a well-defined component of the flow, and submit that component to non-native conditions required for a detection platform of choice, with that detection delivering information about the entire distribution before the partition step, and therefore on the behaviour of the unmodified sample under native conditions. Several detection methods, such as quartz crystal microbalance²⁵ or nanospray mass spectrometry²⁶ can be envisioned. Here, we developed a fluorescence detection platform, because of its rapidity, high sensitivity, low cost, and ease of implementation with standard laboratory instruments.

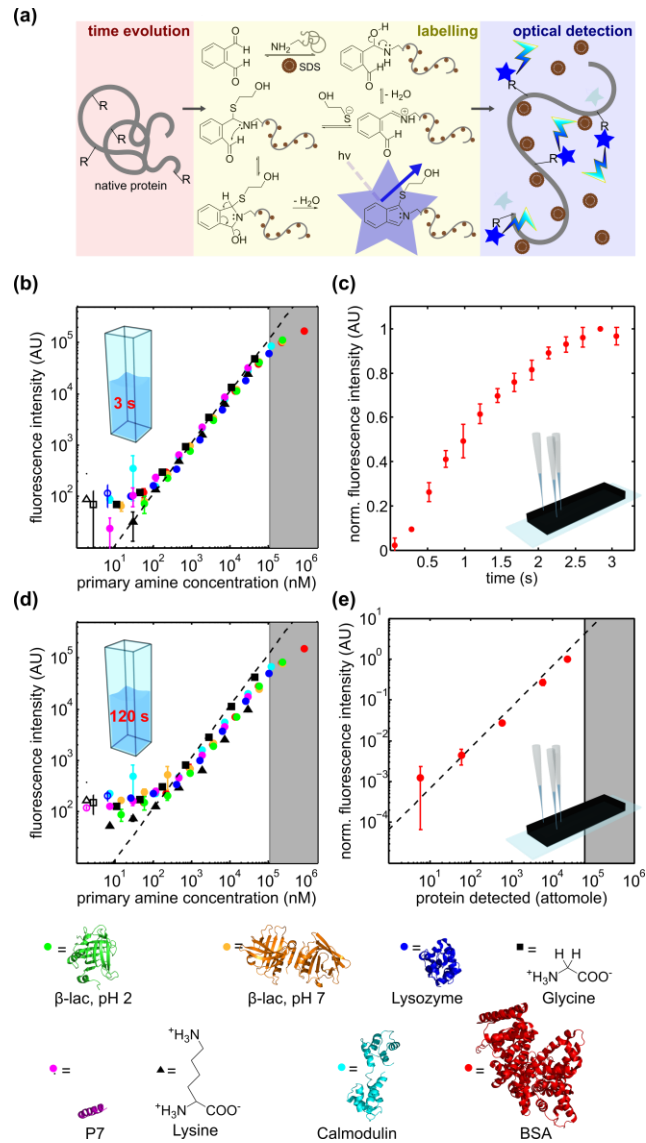


Figure 2: Precise control of reaction time enables quantitative, fluorogenic protein labelling prior to detection. (a) Native proteins are denatured to expose all primary amine (PA) groups within the protein sequence for modification with non-fluorescent OPA. Labelling is quantitative if all, or a constant proportion of, PA groups are modified, such that regardless of sequence or structure, a single linear relationship describes the dependence of the generated isoindole fluorescence intensity (FI) on PA concentration for all of the peptides, proteins, and free amino acids studied (key at bottom). Measurement of FI 3 s (b) after mixing, just after the reaction has reached completion (c), permits accurate determination of ~5 orders of magnitude in protein concentration from FI. Linearity is compromised 120 s after mixing (d) and at later time points (Supp. Figs. 2 & 3). (e) The fluorescence intensity measured after 3 s on chip as a function of protein concentration down to 6 attomole, showing the viability of determining low protein concentrations on a microfluidic chip. Error bars show the SD among independent replicates, data plotted with open markers have been excluded from the fit, and gray shaded areas indicate the range of concentrations over which bulk (b,d) and on-chip (e) absorption measurements are routinely possible (see Supp. Figs. 4 & 5).

Defining the chemical requirements for latent labelling

The conceptual requirement that the total concentration of biomolecules be accessible from measurement of fluorescence intensity alone defines the chemical requirements of the latent labelling module. To permit absolute concentration measurement on chip without the need for calibration, either each biomolecule should be labelled at a single site, or all potential reactive groups within the biomolecule should be modified. Owing to its generality and higher expected signal intensity, we explored the latter quantitative labelling approach, in which the biomolecular concentration can be determined whenever the number of reactive groups within the biomolecule is known. To facilitate quantitative modification and reduce quenching effects, all reactive groups within the biomolecule should be exposed to the solvent. The biomolecule should also be protected against precipitation if it passes through its isoelectric point (IEP) during the labelling step, and the entire process should reach completion on the second to minute timescale, to facilitate real-time readout. The use of a fluorogenic label, which becomes fluorescent exclusively upon reaction with groups of interest within the biomolecule, obviates the need for purification of the labelled biomolecules from the unreacted dye.

We addressed these challenges by adapting the fluorogenic reaction of *ortho*-phthalaldehyde (OPA) with primary amines (PAs).²⁷⁻³¹ Due to the abundance of PA moieties within protein molecules, this method is particularly suited for the determination of low protein concentrations, but any biomolecule containing at least one PA can be analysed. In the presence of compounds with thiol groups such as in β -mercapto ethanol (BME), reaction with a PA group – such as the protein N-terminus, and protein lysine residues – forms a conjugated pyrrole ring, resulting in the formation of a substituted isoindole, giving rise to fluorescence in the blue region of the spectrum.^{29,30} In order to ensure that all PAs are exposed, our procedure involves the addition of high concentrations of sodium dodecyl sulfate (SDS) and excess reducing agent, conditions that are designed to denature the proteins at alkaline pH (10.5)³² (**Fig. 2a**).

To assess the extent of reaction, we observed the fluorescence intensity generated upon labelling a set of well-characterized peptides and proteins with varying secondary, tertiary, and quaternary

structures including some of which would have passed through or approached their IEPs during the labelling step (**Fig. 2, key at bottom**). When the fluorescence intensity is plotted as a function of protein concentration, sequence dependent relationships are observed as predicted. **Supp. Fig. 1** shows representative data for bovine serum albumin (BSA), lysozyme (Lys), and β -lactoglobulin (β -lac). If labelling is quantitative, however, such sequence dependent variation should disappear when fluorescence intensity is instead plotted as a function of the concentration of reactive groups, i.e. PAs. The fluorescence intensity of each protein within the reference set should then fall on a single line, passing through the origin, that also describes the fluorescence intensity of free glycine and lysine. These amino acid controls are small molecules which are chemically similar to the labelled groups but which are solvent accessible without denaturation.

Because the isoindole fluorophore formed during the labelling reaction lacks chemical stability,³³⁻³⁵ extraction of quantitative information from this labelling technique under microfluidic conditions requires that the fluorophore is continuously generated under flow and measured at a defined time after mixing. We examined the dependence of isoindole fluorescence intensity on PA concentration when our reference set of proteins and amino acids was measured 3 s after mixing (**Fig. 2b**), the time we had determined was required for the reaction to reach completion on a microfluidic chip (**Fig. 2c**). Indeed, a single linear relationship described the dependence of fluorescence intensity on PA concentration over a range of more than three orders of magnitude in PA concentration, which corresponds to nearly five orders of magnitude in protein concentration. The fit is fluorescence = 1.11(PA concentration) with $R^2 = 0.91$ (see online methods), and variation in labelling efficiency with protein sequence or among the amino acids controls is not observed.

Precise control over the reaction time, as is accessible via a microfluidic platform, is crucial. When the fluorescence intensity was instead measured at the 120 s time point, we observed deviations from linearity at high and low protein concentrations, as well as substrate-dependent variations in labelling efficiency (**Fig. 2d**). The fit is fluorescence = 1.16(PA concentration), $R^2 = 0.72$. We investigated the reason for these deviations and found that though fluorescence is rapidly generated upon mixing, at later time points fluorescence intensity generally decreased in a complex substrate

and concentration dependent manner (**Supp. Figs. 2 & 3**), consistent with the reported differences in the degradation rates for isoindole fluorophores formed via reaction with varying substrates.^{34,35}

Measurement at the optimised 3 s time point, which was used for the remaining experiments in this paper, allowed for the determination of protein concentrations as low as 1 nM (**Fig. 2b**). This result corresponds to the measurement of approximately 2000 times less than the concentration of protein which can be routinely measured via absorption (**Supp. Fig. 4**). We note that if the study of protein concentrations exceeding the linearity limit is desired, the volumetric mixing ratio of the dye and protein streams can be altered, or a rapid on-chip dilution module can be incorporated.³⁶

Given the low path lengths characteristic of microfluidic systems, we additionally explored the detection limit accessible on the diffusional sizing device (**Fig. 1b**), using BSA as a test system. We measured the fluorescence signal on chip for between 3.75 nM and 15 μ M of this protein, as shown in **Fig. 2e**, suggesting a detection limit in the low nM range. Given that the volume of the portion of the detection region in which fluorescence intensity is quantified in the microfluidic device (**Fig. 1b & Supp. Fig. 7**) is 1.6 nL, this is equivalent to the quantification of on the order of 10^{-17} mol (10 attomole) protein on our chips.

Accurate protein sizing with high dynamic range

Molecular size is calculated based on simple measurements of fluorescence intensity. Quantitative labelling ensures that absolute protein concentration can be determined from measurement of fluorescence intensity within the detection region. Because the system is at steady state, measurement of the protein concentration downstream of the latent labelling module reveals the total concentration of the protein diverted for labelling at time t_D (**Figs. 3a & Fig. 1b**, yellow rectangles); since the microfluidic system is time independent, it is possible to increase the integration time so as to permit detection of very low concentrations of biomolecules.

So as to improve the robustness of the fluorescence intensity quantification against well-known effects such as variation in the illumination source intensity over time,³⁷ a second measurement is taken of a homogeneous reference distribution. Practically, this calibratory measurement can be

made most readily by simply loading the same analyte solution into both the ‘biomolecule’ and ‘buffer’ inlets shown in **Fig. 1b**. Species of varying R_H (indicated colorimetrically) differ in the fraction of diffusing species compared to homogeneously distributed (**Fig. 3a**, black line) species that are diverted for labelling. This is assessed experimentally by comparing the fluorescence intensities for these species in the detection region of the device (**Fig. 3a, inset**). Considering the total volume of protein flowing through the device during the measurement (diffusion + labelling + integration time) for the sample and the homogeneously distributed reference molecules reveals that on the order of one femtomol of protein is required for a sizing measurement, though miniaturization of the device could reduce this requirement even further.

In order to assess the accuracy of the R_H values obtained with our system, we designed a ‘sizing ladder’ of biomolecules varying by over three orders of magnitude in molecular weight (MW) and including, in order of increasing R_H : lysine, a heterogeneous mixture of insulin monomer and dimer, β -lac dimer, intrinsically disordered α -synuclein, BSA, a covalent BSA dimer, and β -galactosidase tetramer. The set of molecules included proteins which differ in secondary and tertiary structure, are natively unfolded as well as folded, and exist as monomeric species or as complexes. In **Fig. 3b**, we compare the results we obtained to those reported in the literature using two established methods for measuring the R_H values of unlabelled proteins (see also Supp. Table 1 for literature references). Pulsed-field gradient NMR (PFG-NMR) was used for low MW weight species with low extinction coefficients, and analytical ultracentrifugation (AUC) for higher MW weight species. Both values were reported where possible. We found that the R_H values obtained with microfluidics agreed closely with those obtained from the composite of AUC and PFG-NMR techniques over the entire MW range studied. The R_H values obtained with microfluidics were also consistently more accurate than MW-based predictions of molecular size (**Supp. Fig. 8**). The accuracy of our method was particularly evident in our analysis of α -synuclein, an intrinsically disordered protein implicated in Parkinson’s disease. We found that the microfluidic R_H value obtained for α -synuclein was consistent with that obtained via PFG-NMR,⁴² and that both were larger than that obtained with AUC,⁴³ a result which is expected because the natively unfolded

structure of α -synuclein is not compact and would be expected to sediment more slowly.

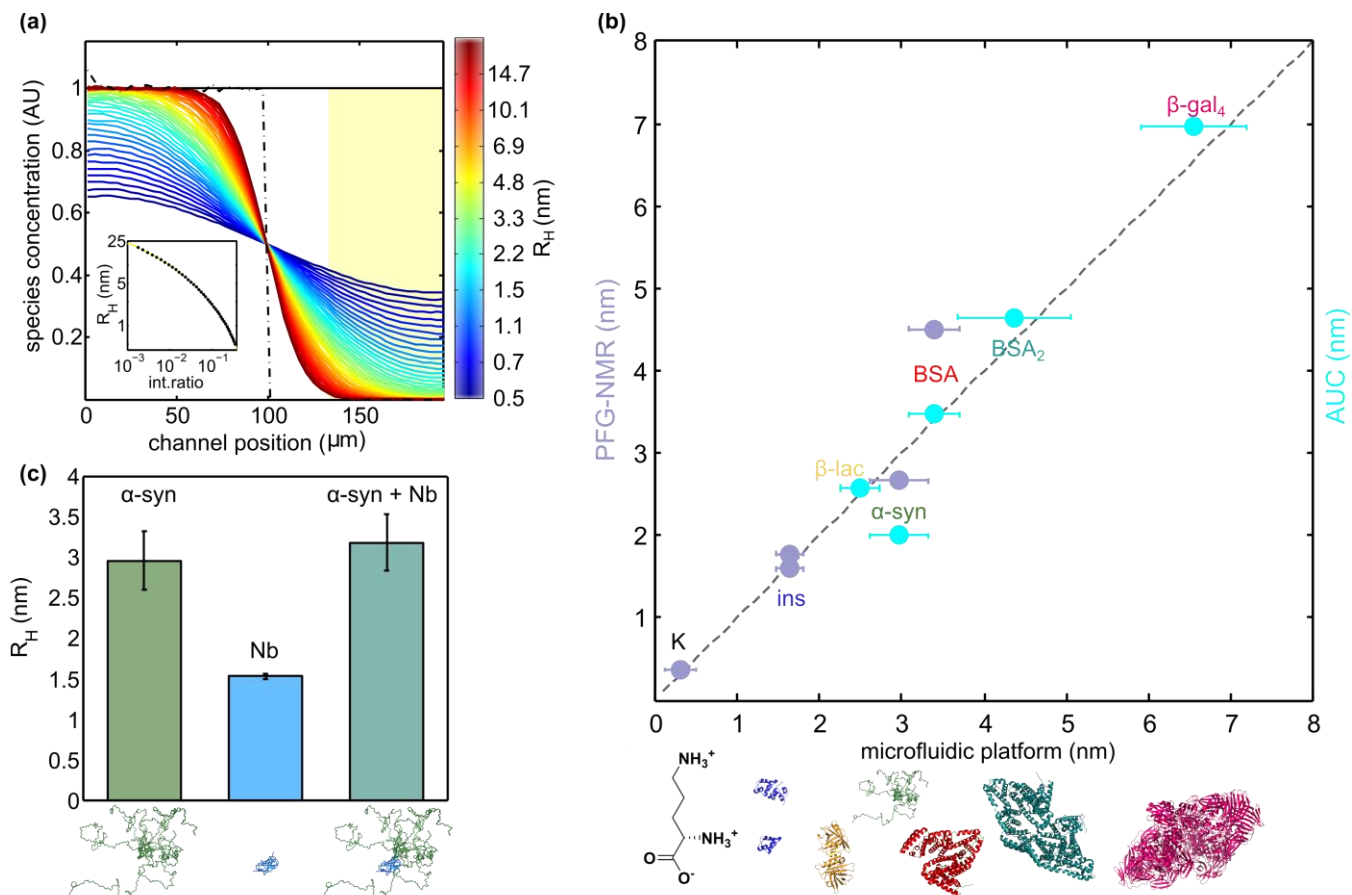


Figure 3: Sizing proteins, heterogeneous mixtures, and protein complexes. (a) Concentration profiles simulated for reference species of known size (Müller *et al*, submitted for publication), viewing laterally across the diffusion channel shown in Fig. 1b. While homogeneously (black horizontal line) and initially (black dashed line) distributed species of all sizes have the same profiles, after diffusion these are determined exclusively by species R_H , indicated colorimetrically. R_H determination involves comparing the total concentrations of diffused versus homogeneously distributed species selected for labelling (yellow shaded area), as shown in inset. (b) R_H values determined in this manner are compared to those obtained with PFG-NMR (lilac) and AUC (aqua) (see also Supp. Table 1). Molecules studied vary by over three orders of magnitude in molecular weight and include intrinsically disordered proteins and heterogeneous mixtures. (c) We exploit this heterogeneous mixture tolerance and accurate sizing of disordered, as well as folded, structures to characterise a novel Parkinson's-related immune complex between a nanobody and equimolar ($5 \mu\text{M}$) α -synuclein, by characterising the hydrodynamic radii of all components. Our data suggest that the nanobody interacts with α -synuclein monomer. The schematic is based on the known locations of a related nanobody's interaction³⁸ with an ensemble representing intrinsically disordered conformations of α -synuclein.³⁹⁻⁴¹ Throughout error bars represent the SD among independent replicates.

Characterising native protein-protein interactions

Having established the sensitivity and accuracy of the system, we additionally explored its tolerance of heterogeneous mixtures. The bovine insulin hormone has been studied extensively *in vitro*, where at low pH and in the absence of Zn^{2+} , the monomer and dimer predominate. Its well-defined oligomers have been characterised hydrodynamically and thermodynamically, so we chose this system to explore whether the composite hydrodynamic radii we obtained reflect the radii expected based on the relative abundance of each species present in the mixture. At pH 2 and in the absence of Zn^{2+} , an association constant of $1.1 \times 10^4 M^{-1}$ has been reported,⁴⁴ which should under the conditions of this study result in 71% insulin monomer and 29% insulin dimer. The R_H of 1.64 nm obtained with native microfluidic diffusional sizing, reflects the proportions of monomer and dimer – which have R_H of 1.60⁴⁵ and 1.78 nm⁴⁶ respectively – present in the sample.

Finally, we made use of this heterogeneous mixture tolerance to additionally explore the use of this procedure to, as proof of concept, characterise an undescribed protein-protein interaction. We chose to study an interaction between α -synuclein and a single-domain camelid antibody, termed a nanobody.⁴⁷ Due to their small size and high stability and specificity, nanobodies are rapidly emerging as important research tools in structural biology and medicine, including their particular use as diagnostic markers and therapeutics for protein misfolding diseases.^{48,49} We have developed nanobodies to study the misfolding of several proteins, and have shown that the nanobody NbSyn2³⁸ can be used as a molecular probe for the detection of subtle conformational differences upon α -synuclein fibril maturation.⁵⁰ Due to the conformational flexibility of intrinsically disordered α -synuclein, the characteristics of the labelled complex may be expected to differ significantly from that of the native, unmodified system.

We used the microfluidic platform to explore the binding of α -syn to a variant of NbSyn2, NbSyn1³⁸. Our approach involved characterising the hydrodynamic radii of all components (**Fig. 3c**). If NbSyn1 binds to the alpha-synuclein monomer, under conditions such as those explored

here in which the system would be expected to be fully bound based on the dissociation constants of related mutants, then the predicted size increase on binding can be calculated based on the change in molecular weight on complex formation, using a MW based prediction of molecular size (as described in **Supp. Fig. 8**). Our prediction corrects for the larger than ‘minimum’ R_H observed for α -synuclein in isolation due to its intrinsically disordered structure by taking into account an adjusted molecular weight which would be expected for a protein with the measured R_H . In this manner the size of the bound complex is predicted to be 3.11 nm, which is in accord with the measured 3.10 ± 0.35 nm, and suggests that NbSyn1 indeed binds to the alpha-synuclein monomer. By contrast, binding to an oligomeric species would require a complex size of at least 3.82 nm, which is not observed. Thus, this approach reveals not only that a binding event has occurred, but also suggests the oligomerisation state of the target, which is frequently, as in the Parkinson’s-associated system studied, a crucial determinant of its biological activity.⁶

Native microfluidic diffusional sizing has a series of distinctive features relative to conventional methods, such as SPR and ITC, for characterizing this type of complex: measurements are rapid, entirely in the solution phase, tolerant of any desired buffer conditions as long as the only primary amines are those intended for detection, consume only μL of sample, can probe interactions that are entropically as well as enthalpically driven, and the direct output of the measurement is a fundamental physical property – molecular dimension, which gives additional information about the oligomerisation state of the target.

Conclusions

In summary, the development of methods enabling the characterisation of native, unmodified biomolecules and their complexes in the solution phase is of central significance in structural and functional biology. The data presented here demonstrate that, by integrating chemical and physical tools to create a latent analysis approach, our technology makes it possible to achieve highly sensitive (attomole) detection sensitivity of native proteins. Indeed, species ranging in size

from individual amino acids (146 Da) to large protein complexes (464000 Da) could be accurately sized. This method is applicable to intrinsically disordered proteins and heterogeneous mixtures and has key advantages over existing technologies. Principally, it is a non-disruptive, solution phase method that enables characterisation of low concentrations of biomolecules and their interactions, without the need for prior labelling. This is important because if prior labelling is used to enhance detection it can both perturb the behaviour under observation and require significant researcher effort to identify conditions which may lessen this perturbation. Indeed, due to its simplicity and generality we expect that this technology, and other latent analysis approaches in which the behaviour of unmodified biomolecules is measured with high sensitivity, will be of particular relevance in the study of the strength and kinetics of protein-protein and protein-nucleic acid interactions which are increasingly recognized as the next generation of pharmaceutical targets,⁸ as well as in the characterisation of protein and protein complex interactions with small molecule modulators.

Methods

Bulk labelling measurements

A variety of fluorogens, stoichiometries, and denaturing conditions were investigated using a fluorescence spectrometer (Varian, Cary Eclipse) and fluorescence microplate reader (BMG LabTech), in quartz fluorescence cuvettes (Hellma), or half-area non-protein binding microplates (Corning, product #3881), respectively. The quantitative labelling cocktail described in this paper was composed of: 12 mM OPA, 18 mM BME, and 4% w/v SDS in 200 mM carbonate buffer, pH 10.5. Generally, 16 mg OPA was dissolved in 4 mL 500 mM carbonate buffer, pH 10.5. Then 12.63

μ L BME was added, along with 4 mL water, and 2 mL of a 20% w/v solution SDS. The cocktail was protected from light and heated at 65 °C for 10 minutes, or until the OPA dissolved, then allowed to cool to room temperature and filtered. Labelling solutions were protected from light at room temperature, and used within five days of preparation, or frozen and used within fourteen days of preparation. The solutions were standardly mixed in 1:1 v/v with each of the samples of interest. Unless otherwise stated, protein solutions were prepared in 5 mM HEPES, pH 7.0, and their concentrations determined spectrophotometrically on a NanoDrop UV-Vis spectrophotometer (Thermo Scientific, Willmington, DE, USA).

Time controlled fluorescence measurements were performed using a CLARIOstar microplate reader (BMG LabTech) fitted with an injector module. The measurements were performed in ‘well mode,’ meaning that each well was treated separately. The injector module delivered 50 μ L dye into a single well at a speed of 430 μ L/s, agitated the plate for 1s, and then measured the sample every 0.25 s for a duration of 125 s, before moving on to the next well. Every sample and dye background solution was prepared in triplicate.

For a discussion of microfluidic design and fabrication, see the online supplementary information

Microfluidic measurements

Devices were loaded by first filling all channels from the outlet with the appropriate buffer. The buffer and samples were filtered through a 0.22 μ m filter (Millipore) immediately prior to use, to eliminate particulate matter which could clog the devices. Generally, either a 1 mL Hamilton glass syringe, or a 1 mL plastic Air-Tite syringe, connected through a 27 gauge needle to portex tubing was used. No differences were noted between the performance of glass and plastic syringes at the flow rates used in these experiments. Pressure was then applied simultaneously at the inlets and through the syringe to remove any bubbles formed during the loading process, and reagents were introduced with gel loading tips at the device inlets. Reagent loading varied between 10 and

200 μL , depending on the nature of the particular experiment, though even smaller volumes can be used.

Fluid was withdrawn through the device with a neMESYS syringe pump. In order to draw reagents through the device initially and minimize the effects of any inlet cross-flow during the loading step, 20 μL fluid was first withdrawn at a flow rate of 300 $\mu\text{L}/\text{hr}$. For the microfluidic device used in these experiments, a 25 $\mu\text{L}/\text{hr}$ flow rate in the diffusion chamber was selected, which corresponded to a 33.3 $\mu\text{L}/\text{hr}$ withdrawal rate at the outlet. The flow rate was allowed to equilibrate for at least 18 min prior to the start of image acquisition, and for at least 500 s following sample changes. The initial equilibration steps can be performed with buffer to reduce sample consumption. An efficient sample change procedure involved depositing a drop of buffer around the gel-loading tip that delivered the sample into the indicated inlet, then rapidly removing that tip and replacing it drop-to-drop with a second tip filled with the new sample, all the while withdrawing at the desired flow rate.

Brightfield and fluorescence images were acquired using a Zeiss AxioObserver Microscope, fitted with an Evolve 512 CCD camera (Photometrics), and a 365 nm Cairn OptoLED and DAPI filter (product # 49000, Chroma, Vermont USA) for the fluorescence images. 2.5X, 5X, 10X, and 20X objectives were used, and exposure times of between 10 ms and 10 s were used; generally between 10 and 60 images were averaged during each acquisition. When the signal intensity was low, EM gain was used, or adjacent pixels were binned. For each set of measurements, at least one dye background image was taken to account for the (minimal) fluorescence of the unreacted dye. A flatfield background image was also acquired, and measurements were taken in a dark environment, with the temperature maintained at 25 °C.

Competing financial interests

Part of the work described here has been the subject of a patent application filed by Cambridge Enterprise Ltd, a fully owned subsidiary of the University of Cambridge (now licensed to Fluidic Analytics, of which C.M.D. is a scientific advisor and T.P.J.K. is a board member).

Author contributions

T.P.J.K. and C.M.D. supervised the research. E.V.Y., L.R., M.V., C.M.D, and T.P.J.K conceived of and designed the experiments. E.V.Y. performed the experiments. E.V.Y. and T.M. analysed the data. E.J.D.G., P.A., and S.L. contributed materials and/or analysis tools. E.V.Y., C.M.D., and T.P.J.K. wrote the paper, and all authors commented on the paper.

Acknowledgement

We would like to thank the ERC, BBSRC, Wellcome Trust, Newman Foundation, Winston Churchill Foundation, and Elan Pharmaceuticals for financial support. E.D.G was supported by the MRC (G1002272). We would further like to thank Prof. Jan Steyaert at the Free University of Brussels for sharing the NbSyn1a clone.

Bibliography

- (1) Balch, W. E.; Morimoto, R. I.; Dillin, A.; Kelly, J. W. Adapting Proteostasis for Disease Intervention. *Science* **2008**, *319*, 916–919.
- (2) Suh, E. H.; Liu, Y.; Connelly, S.; Genereux, J. C.; Wilson, I. A.; Kelly, J. W. Stilbene Vinyl Sulfonamides as Fluorogenic Sensors of and Traceless Covalent Kinetic Stabilizers of Transthyretin That Prevent Amyloidogenesis. *Journal of the American Chemical Society* **2013**, *135*, 17869–17880.
- (3) Aguzzi, A.; Calella, A. M. Prions: Protein Aggregation and Infectious Diseases. *Physiological Reviews* **2009**, *89*, 1105–1152.
- (4) Campioni, S.; Carret, G.; Jordens, S.; Nicoud, L.; Mezzenga, R.; Riek, R. The Presence of an Air-Water Interface Affects Formation and Elongation of α -Synuclein Fibrils. *Journal of the American Chemical Society* **2014**, *136*, 2866–2875.
- (5) Adamcik, J.; Jung, J.-M.; Flakowski, J.; De Los Rios, P.; Dietler, G.; Mezzenga, R. Understanding amyloid aggregation by statistical analysis of atomic force microscopy images. *Nature Nanotechnology* **2010**, *5*, 423–428.
- (6) Chiti, F.; Dobson, C. M. Protein Misfolding, Functional Amyloid, and Human Disease. *Annual Review of Biochemistry* **2006**, *75*, 333–366.
- (7) Arkin, M. R.; Whitty, A. The road less traveled: modulating signal transduction enzymes by inhibiting their protein–protein interactions. *Current Opinion in Chemical Biology* **2009**, *13*, 284–290.
- (8) Wells, J. A.; McClendon, C. L. Reaching for high-hanging fruit in drug discovery at protein-protein interfaces. *Nature* **2007**, *450*, 1001–1009.
- (9) Berggård, T.; Linse, S.; James, P. Methods for the detection and analysis of protein–protein interactions. *PROTEOMICS* **2007**, *7*, 2833–2842.

- (10) Uetz, P. et al. A comprehensive analysis of protein-protein interactions in *Saccharomyces cerevisiae*. *Nature* **2000**, *403*, 623–627.
- (11) Ho, Y. et al. Systematic identification of protein complexes in *Saccharomyces cerevisiae* by mass spectrometry. *Nature* **2002**, *415*, 180–183.
- (12) Yu, X.; Xu, D.; Cheng, Q. Label-free detection methods for protein microarrays. *Proteomics* **2006**, *6*, 5493–5503.
- (13) Zuiderweg, E. R. P. Mapping Protein-Protein Interactions in Solution by NMR Spectroscopy. *Biochemistry* **2001**, *41*, 1–7.
- (14) Hanlon, A. D.; Larkin, M. I.; Reddick, R. M. Free-Solution, Label-Free Protein-Protein Interactions Characterized by Dynamic Light Scattering. *Biophysical Journal* **2010**, *98*, 297–304.
- (15) Lee, T. T.; Yeung, E. S. High-sensitivity laser-induced fluorescence detection of native proteins in capillary electrophoresis. *Journal of Chromatography A* **1992**, *595*, 319–325.
- (16) Bornhop, D. J.; Latham, J. C.; Kussrow, A.; Markov, D. A.; Jones, R. D.; Sørensen, H. S. Free-Solution, Label-Free Molecular Interactions Studied by Back-Scattering Interferometry. *Science* **2007**, *317*, 1732–1736.
- (17) Jungbauer, L. M.; Yu, C.; Laxton, K. J.; LaDu, M. J. Preparation of fluorescently-labeled amyloid-beta peptide assemblies: the effect of fluorophore conjugation on structure and function. *Journal of Molecular Recognition* **2009**, *22*, 403–413.
- (18) Herling, T. W.; Muller, T.; Rajah, L.; Skepper, J. N.; Vendruscolo, M.; Knowles, T. P. J. Integration and characterization of solid wall electrodes in microfluidic devices fabricated in a single photolithography step. *Applied Physics Letters* **2013**, *102*, 184102–4.
- (19) Bruus, H. *Theoretical Microfluidics*; Oxford Master Series in Physics; OUP Oxford, 2008.
- (20) Brody, J. P.; Yager, P. Diffusion-based extraction in a microfabricated device. *Sensors and*

- Actuators A: Physical* **1997**, 58, 13 – 18, Micromechanics Sections of Sensors and Actuators.
- (21) Weigl, B. H.; Yager, P. Microfluidic Diffusion-Based Separation and Detection. *Science* **1999**, 283, 346–347.
- (22) Kamholz, A. E.; Weigl, B. H.; Finlayson, B. A.; Yager, P. Quantitative Analysis of Molecular Interaction in a Microfluidic Channel: The T-Sensor. *Analytical Chemistry* **1999**, 71, 5340–5347.
- (23) Hatch, A.; Kamholz, A. E.; Hawkins, K. R.; Munson, M. S.; Schilling, E. A.; Weigl, B. H.; Yager, P. A rapid diffusion immunoassay in a T-sensor. *Nature Biotechnology* **2001**, 19, 461–465.
- (24) Kamholz, A. E.; Schilling, E. A.; Yager, P. Optical Measurement of Transverse Molecular Diffusion in a Microchannel. *Biophysical Journal* **2001**, 80, 1967 – 1972.
- (25) Knowles, T.; Devlin, G.; Dobson, C.; Welland, M. In *Methods in Molecular Biology*; Hill, A. F., Barnham, K. J., Bottomley, S. P., Cappai, R., Eds.; Humana Press, 2011; Vol. 752; pp 137–145–.
- (26) Gao, D.; Liu, H.; Jiang, Y.; Lin, J.-M. Recent advances in microfluidics combined with mass spectrometry: technologies and applications. *Lab Chip* **2013**, 13, 3309–3322.
- (27) Roth, M. Fluorescence Reaction for Amino Acids. *Analytical Chemistry* **1971**, 43, 880–882.
- (28) Benson, J. R.; Hare, P. o-Phthalaldehyde: Fluorogenic Detection of Primary Amines in the Picomole Range. Comparison with Fluorescamine and Ninhydrin. *Proceedings of the National Academy of Sciences of the United States of America* **1975**, 72, 619–622.

- (29) Simons, S. S.; Johnson, D. F. The structure of the fluorescent adduct formed in the reaction of o-phthalaldehyde and thiols with amines. *Journal of the American Chemical Society* **1976**, *98*, 7098–7099.
- (30) Sternson, L. A.; Stobaugh, J. F.; Repta, A. J. Rational design and evaluation of improved o-phthalaldehyde-like fluorogenic reagents. *Anal Biochem* **1985**, *144*, 233–246.
- (31) Jacobson, S. C.; Koutny, L. B.; Hergenroeder, R.; Moore, A. W.; Ramsey, J. M. Microchip Capillary Electrophoresis with an Integrated Postcolumn Reactor. *Analytical Chemistry* **1994**, *66*, 3472–3476.
- (32) Otzen, D. Protein-surfactant interactions: A tale of many states. *Biochimica et Biophysica Acta - Proteins and Proteomics* **2011**, *1814*, 562–591.
- (33) Stobaugh, J.; Repta, A.; Sternson, L.; Garren, K. Factors affecting the stability of fluorescent isoindoles derived from reaction of o-phthalaldehyde and hydroxyalkylthiols with primary amines. *Analytical Biochemistry* **1983**, *135*, 495–504.
- (34) Lindroth, P.; Mopper, K. High performance liquid chromatographic determination of subpicomole amounts of amino acids by precolumn fluorescence derivatization with o-phthalaldehyde. *Analytical Chemistry* **1979**, *51*, 1667–1674.
- (35) Svedas, V. J.; Galaev, I. J.; Borisov, I. L.; Berezin, I. V. The Interaction of Amino Acids with o-Phthalaldehyde: A Kinetic Study and Spectrophometric Assay of the Reaction Product. *Analytical Biochemistry* **1980**, *101*, 188–195.
- (36) Horrocks, M. H.; Rajah, L.; Jönsson, P.; Kjaergaard, M.; Vendruscolo, M.; Knowles, T. P. J.; Klenerman, D. Single-Molecule Measurements of Transient Biomolecular Complexes through Microfluidic Dilution. *Analytical Chemistry* **2013**, *85*, 6855–6859.
- (37) Waters, J. C. Accuracy and precision in quantitative fluorescence microscopy. *The Journal of Cell Biology* **2009**, *185*, 1135–1148.

- (38) De Genst, E. J.; Guilliams, T.; Wellens, J.; O'Day, E. M.; Waudby, C. A.; Meehan, S.; Dumoulin, M.; Hsu, S.-T. D.; Cremades, N.; Verschueren, K. H.; Pardon, E.; Wyns, L.; Steyaert, J.; Christodoulou, J.; Dobson, C. M. Structure and Properties of a Complex of alpha-Synuclein and a Single-Domain Camelid Antibody. *Journal of Molecular Biology* **2010**, *402*, 326–343.
- (39) Jha, A. K.; Colubri, A.; Freed, K. F.; Sosnick, T. R. Statistical coil model of the unfolded state: Resolving the reconciliation problem. *Proceedings of the National Academy of Sciences of the United States of America* **2005**, *102*, 13099–13104.
- (40) Ulmer, T. S.; Bax, A.; Cole, N. B.; Nussbaum, R. L. Structure and Dynamics of Micelle-bound Human α -Synuclein. *Journal of Biological Chemistry* **2005**, *280*, 9595–9603.
- (41) Dedmon, M. M.; Lindorff-Larsen, K.; Christodoulou, J.; Vendruscolo, M.; Dobson, C. M. Mapping Long-Range Interactions in α -Synuclein using Spin-Label NMR and Ensemble Molecular Dynamics Simulations. *J. Am. Chem. Soc.* **2005**, *127*, 476-477.
- (42) Morar, A. S.; Olteanu, A.; Young, G. B.; Pielak, G. J. Solvent-induced collapse of α -synuclein and acid-denatured cytochrome c. *Protein Science* **2001**, *10*, 2195–2199.
- (43) Weinreb, P. H.; Zhen, W.; Poon, A. W.; Conway, K. A.; Lansbury, P. T. NACP, A Protein Implicated in Alzheimer's Disease and Learning, Is Natively Unfolded. *Biochemistry* **1996**, *35*, 13709–13715.
- (44) Lord, R. S.; Gubensek, F.; Rupley, J. A. Insulin self-association. Spectrum changes and thermodynamics. *Biochemistry* **1973**, *12*, 4385–4392.
- (45) Bocian, W.; Sitkowski, J.; Bednarek, E.; Tarnowska, A.; Kawkecki, R.; Kozerski, L. Structure of human insulin monomer in water/acetonitrile solution. *Journal of Biomolecular NMR* **2008**, *40*, 55–64.
- (46) Lin, M.; Larive, C. Detection of Insulin Aggregates with Pulsed-Field Gradient Nuclear

Magnetic Resonance Spectroscopy. *Analytical Biochemistry* **1995**, 229, 214 – 220.

- (47) Muyldermans, S. Nanobodies: Natural Single-Domain Antibodies. *Annual Review of Biochemistry* **2013**, 82, 775–797.
- (48) De Genst, E.; Messer, A.; Dobson, C. M. Antibodies and protein misfolding: From structural research tools to therapeutic strategies. *Biochimica et Biophysica Acta - Proteins and Proteomics* **2014**, 1844, 1907–1919.
- (49) De Genst, E.; Dobson, C. M. *Methods in Molecular Biology*; 2012; Vol. 911; pp 533–558.
- (50) Guilliams, T.; El-Turk, F.; Buell, A. K.; O’Day, E. M.; Aprile, F. A.; Esbjörner, E. K.; Vendruscolo, M.; Cremades, N.; Pardon, E.; Wyns, L.; Welland, M. E.; Steyaert, J.; Christodoulou, J.; Dobson, C. M.; De Genst, E. Nanobodies Raised against Monomeric α -Synuclein Distinguish between Fibrils at Different Maturation Stages. *Journal of Molecular Biology* **2013**, 425, 2397–2411.